

# Reactive Inkjet Printing Applications for Tissue Engineering

Christopher Tse, Patrick J. Smith; University of Sheffield, Sheffield, UK

## Abstract

A crosslinking agent (glutaraldehyde) was selectively inkjet printed at predetermined locations onto a sheet of virgin gelatin and washed to create biocompatible scaffolds of bespoke shapes. Fibroblasts were seeded onto these scaffolds and were shown to proliferate with no detrimental effects for 3 days compared to controls. This method of creating biocompatible scaffolds takes advantage of inkjet printing's ability to create complicated designs without compromise at a range of fibre diameters from as thin as 80µm. Fibroblasts were seen to cover the entire surface. Future research will be focused on using such technology in nerve repair.

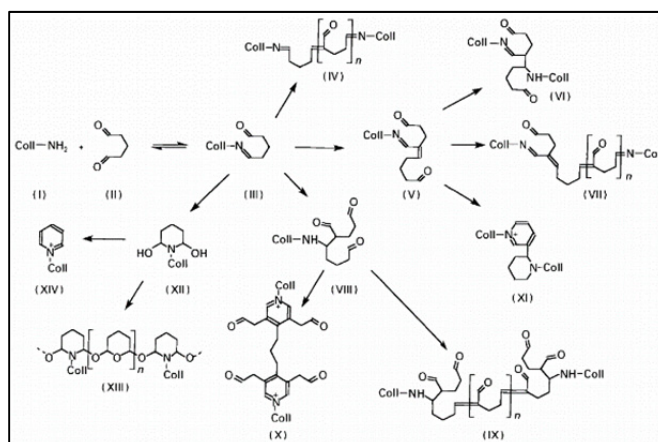
## Introduction

Research into cell patterning and spatial coordination are growing fields, as new technologies enable researchers to accurately position populations of cells and promote the design of better biological systems.[1]–[3] When considering the design of cell patterning experiments, geometry and topology are important factors that affect anchorage-dependent cells,[4]–[7] as living cells actively investigate their surroundings, which can influence function and morphology.[8] The wealth of knowledge that can be generated through studying cell-to-cell behaviour and cell-to-substrate interactions can allow scientists to better understand the dynamic mechanism that affects cell architecture, polarity, morphology, survival and division within their surrounding environments.[4], [9]–[11]

Gelatin is one of the most commonly used hydrogels for mammalian cell growth[12] and biomedical applications. Such biomedical applications include drug delivery through hard and soft capsules, wound dressings, cell encapsulation and in vitro tissues [13]–[15]. Gelatin is a biocompatible denatured protein of collagen that is biodegradable, non-immunogenic and can be controlled at a desired rate by altering the cross-linking to suit its purpose. Cross-linking of the biopolymer is required as virgin gelatin turns into its sol state at biological temperatures (37°C), which upon cooling returns to a thermoreversible hydrogel.

Transglutaminase,[16], [17] genipin,[18], [19] formaldehyde,[20] carbodiimides,[21] riboflavin[22] and glutaraldehyde[23], [24] have been researched extensively as crosslinking agents for gelatin. All crosslinking agents offer a degree of toxicity, and although glutaraldehyde has been shown to cause the most cell death as a crosslinking agent, glutaraldehyde provided the best mechanical strength and was selected.

Crosslinking of gelatin by glutaraldehyde occurs through the aldehyde groups reacting to the free amino groups of lysine or hydroxylysine amino acid residues on gelatin molecules.[25] Primary amines and secondary amines react with the aldehyde group in glutaraldehyde through nucleophilic addition to form carbinolamines, which can then dehydrate to give substituted imines and enamines respectively. A range of possible resultant products are outlined in Scheme 1. This diagram shows collagen reacting with glutaraldehyde. Many of the reactions involve the formation of a Schiff base intermediate (Structure III) that is able to form a plethora of products. It is through this reaction that the mechanical properties of gelatin and its mechanical properties increase; through the generation of bigger complex compounds within the gelatin.



**Scheme 1.** Gelatin is denatured collagen, and the various reactions pathways shown here can be related to the crosslinking of gelatin (i.e. Coll-NH<sub>2</sub> = Collagen-amine group). Taken from Damink et al. 1995.[26]

Much has been learnt recently about cell behaviour in a micro-environment and the creation of microstructures, that are essential in the understanding of fabricating micro-devices to control cell-substrate interactions.[27]–[30] The importance of such research was highlighted in a special themed issue of *Soft Matter* in 2014 on cells in patterned environments.[31] Being able to control the fabrication of biocompatible scaffolds and able to seed cells thereafter allows the creation of scaffolds suitable for tissue engineering, biosensors, the formation of neuronal networks, cell-based assays and for the study of cell-cell interactions.

## Results and Discussion

25% glutaraldehyde (in distilled water) was inkjet printed onto 4% (w/v) gelatin of various shapes, to create the most structurally stable scaffolds (Figure 1).

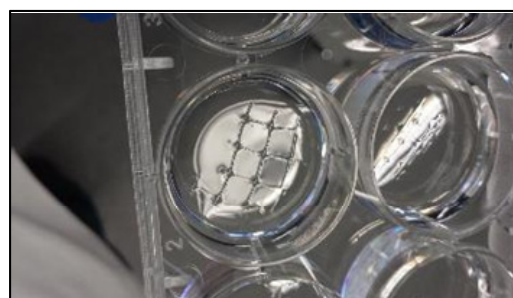


**Figure 1** Crosslinked gelatin patterns created with an inkjet printer. 25% glutaraldehyde was printed onto a bed of 4% gelatin with a droplet spacing of 100 µL, left for 24 hours for crosslinking to take place, and then compartmentalised in well plates prior to washing with 50°C distilled water five times to remove uncrosslinked gelatin and residual glutaraldehyde.

The resultant crosslinked gelatin structures were handled successfully and fibroblasts were seeded into the scaffolds. Fibroblasts were able to grow on the patterned environments on all days that they were observed (day 1, 2 and 3 after cell seeding). Figure 2 shows an example of images taken of the scaffolds seeded with fibroblasts. The structure appears “furry” due to the surface of the hydrogel being populated by

fibroblasts. Seeded fibroblasts proliferated at a rate that is typical for healthy cells, as can be seen under the microscope. If the scaffolds did release glutaraldehyde, or it was detrimental to cell health, the population of cells would have decreased on the scaffold, or more cells would adopt a spherical shape to indicate unfavourable culture conditions and undergo apoptosis. These types of physical cues were not seen in all samples examined.

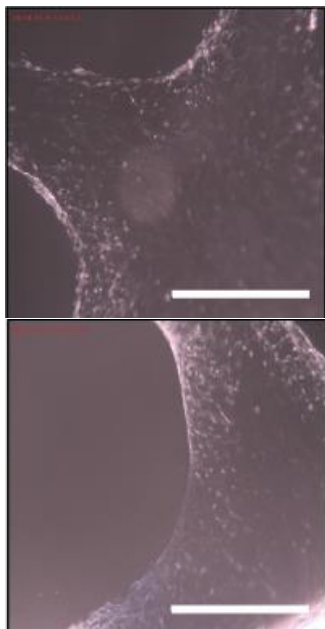


**Figure 2** Microscopy images of fibroblasts seeded onto crosslinked gelatin through inkjet printing glutaraldehyde onto a bed of gelatin. Images taken 1 and 3 days after cell seeding respectively. Scale bar = 300  $\mu$ m

The gelatin scaffolds that were created had a range of thicknesses, ranging from 250-100  $\mu$ m, being thickest at the intersections. The beams resembled a more cylindrical shape, which was caused by the way in which the glutaraldehyde diffused uniformly from the area of deposition. Figure 3 shows enlarged light microscopy images of the cell seeded gelatin scaffolds.

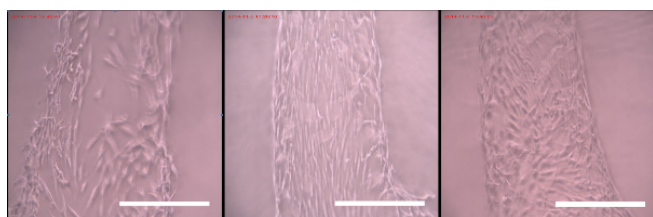


**Figure 3.** Enlarged microscopy images of fibroblasts seeded onto crosslinked gelatin through inkjet printing. Images taken 1, 2 and 3 days after cell seeding respectively. Scale bar = 150  $\mu$ m

On day 1 after cell seeding, cells manage to adhere and begin to proliferate on the scaffold. There is a larger population of cells proliferating on the side of the scaffold that was facing the cell seeding process, but it is interesting to see cells have also managed to grow on the periphery and underside of the scaffold.

By day 2 and 3, as shown in Figure 3 there are no detrimental effects of crosslinking with glutaraldehyde, cells have proliferated along the whole structure. More alignment of the cells can be seen on day 2, that are running in the same direction as the beams. The alignment was lost once the population of fibroblasts become overconfluent growing on the scaffold.

Confocal images were recorded to analyse the cell seeded gelatin scaffolds. Due to the 3D nature of the scaffold, the confocal images capturing a plane of the scaffold show a limited amount of data. However, the details that can be seen by analysing each pane individually makes it clear that some fibroblasts were able to infiltrate into the scaffold and proliferate within. Figure 4 shows a cross-section of a gelatin scaffold seeded with fibroblasts after 3 days of cell seeding. The periphery of the image shows a row of cells on the surface of the gelatin scaffold; stained for actin (red; phalloidin-FITC) and nuclei (blue; DAPI), and also note the cells situated in the middle of the image. These cells are proliferating within the gelatin scaffold, and it is that the fibroblasts were able to not just proliferate on the surface of the gelatin, but also infiltrate inside the hydrogel.

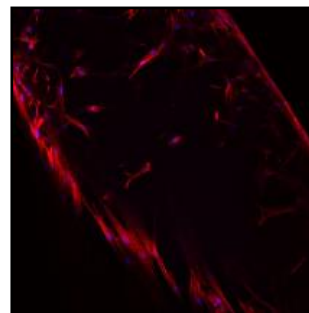


**Figure 4** Confocal image of a cross-section of the middle of a gelatin scaffold beam stained for actin (red; phalloidin-FITC) and nuclei (blue; DAPI)

Several areas were analysed, and a z-stack was created of each area. By combining the z-stack images with the Zeiss LSM Image Browser software, a 3D model of the scaffold was created. The majority of cells that proliferate on the scaffolds were proliferating on the surface. A small percentage of fibroblasts were growing within the gelatin hydrogel, and this population increased over time. Most cell proliferation occurred on the outside of the scaffold, as it was most likely caused by the cells preferentially proliferating to areas with the least resistance. It could be seen that there were more cells infiltrating the hydrogel during the second and third day after cell seeding, as the surface of the gelatin become more populated, the action of proliferating through the gelatin hydrogel became a better alternative than competing for space on the outer surface.

The morphology of the gelatin scaffolds varied over time; as originally, the branches were typically cylindrical in shape. With the addition of cells, they are able to degenerate the gelatin slowly, and when the cell population on the gelatin become confluent, the gelatin scaffolds became more elongated and flat. Figure 5 shows the flattening of the gelatin occurring after 3 days after cell seeding.

In the target area, cells had fully covered the surface facing the cell seeding side, and cells had begun migrating into and enveloping the scaffold. The shape of the gelatin scaffold can be determined through the outlines given by the population of cells adhering onto and into the scaffold. More cells can be seen proliferating within the hydrogel compared to samples analysed on day 1 after cell seeding.

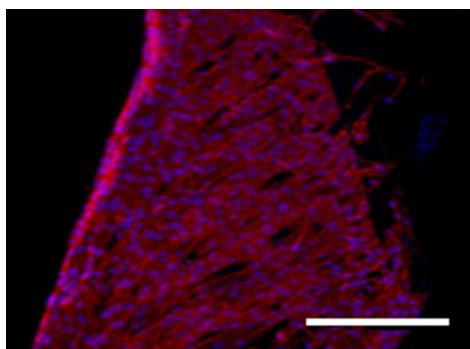


**Figure 5** fibroblasts grown on glutaraldehyde-crosslinked gelatin. A 3D image was generated through the stacking of multiple confocal images to create a z-stack. Stained for actin (red; phalloidin-FITC) and nuclei (blue; DAPI), day 3 after cell seeding. Cells proliferated significantly more on the surface side where cell seeding took place. Cells can be seen to infiltrate within the gelatin and grow within the scaffold. Scale bar = 250  $\mu$ m.

## Conclusion

The use of inkjet printing provides a method to create biocompatible scaffolds that are beneficial to tissue engineering. Cross-hatched and linear scaffolds were created with this technique and seeded cells shown to proliferate and align with the scaffold orientation, with this alignment becoming noisier through time due to over-confluency on the structures (Figure 3). Thinner scaffolds could be created with a lower concentration of glutaraldehyde, however more care must be taken to prevent accidental damage to the scaffolds through handling them. Preliminary experiments had shown that crosslinked gelatin scaffolds created with glutaraldehyde concentrations of 10 and 15% produced scaffolds that were too fragile and irrevocably damaged during the transportation of the scaffolds from one well plate to another for experimentation.

The high concentration of glutaraldehyde that was used did not cause the gelatin scaffold to become toxic, as it can be assumed that all glutaraldehyde molecules were either fully reacted with the gelatin, and/or all residual glutaraldehyde was removed during the washing process. Inkjet printing is able to create biocompatible scaffolds.

Thicker scaffolds could be created by the printing of multiple layers of glutaraldehyde onto the bed of gelatin; however like all other tissue engineered scaffolds, all scaffolds that do not exceed a few millimetres in thickness can have cells proliferate on/in them, as simple diffusion is a sufficient method to transport nutrients into cells from the cell media and remove waste. A limit to inkjet printing would be that scaffolds may not be more than a few millimetres thick, unless a vasculature network is designed within the scaffold to allow directed transport of nutrients and cell waste throughout the scaffold. It could be postulated that with the simple cross hatch pattern that was used to create these scaffolds, once cells have been seeded, the scaffold could be collapsed and rolled together to form a larger, thicker scaffold of significant size, and with the porosity of the design of the scaffold, cells would survive at a better rate than a solid block of hydrogel of the same material.

## Experimental

A Jetlab 4 xl-A tabletop-printing platform single nozzle piezoelectric inkjet device (MicroFab, Texas, USA) was used, equipped with drop-on-demand PH-46 printheads (MicroFab, Texas, USA). A CT-PT4 four channel pressure controller was used (MicroFab, Texas, USA) to maintain a slight negative pressure within the system to control a nozzle meniscus level for optimal jetting. A JetDrive III was used to control the generation of a waveform and tailor the jetting parameters to the printheads.

Prior to jetting, all tubing, reservoirs and printheads were flushed with 1% (v/v) Micro-90 cleaning solution (10 mL for 10 minutes), distilled de-ionised water (20 mL for 30 minutes) and subsequently with cell culture medium (DMEM / 10% foetal calf serum (FCS)). The inkjet printer was calibrated to print the glutaraldehyde at 80 V, rise time 36  $\mu$ s, dwell time 42  $\mu$ s, fall time 50  $\mu$ s and printed within 3 mm from the surface of the substrate.

The scaffolds used for cell seeding were made by printing 25% glutaraldehyde (25% in distilled water, G6257, Sigma, UK) in a cross hatch pattern onto 4% gelatin (v/v in distilled water) on glass slides and reacted for 24 hours before the removal of uncrosslinked gelatin. The scaffolds were washed five times with 50°C water to remove uncrosslinked gelatin and residual glutaraldehyde and left soaking for 1 hour prior to cell seeding. This washing removed uncrosslinked gelatin and excess residual glutaraldehyde from the sample.

Human dermal fibroblasts were obtained from abdominoplasty or breast reduction operations according to local ethically approved guidelines (under an HTA Research Tissue Bank license number 12179).

Cells were cultured in a humidified 37°C/5% CO<sub>2</sub>/95% air (v/v) environment in Dulbecco's modified Eagle's medium (DMEM; Sigma) containing 10% (v/v) FCS (Gibco, UK), 1% (v/v) L-glutamine (Gibco, UK), 1% (v/v) penicillin/streptomycin (Gibco, UK), and 0.5% (w/v) amphotericin B (Gibco, UK). Porcine Schwann cells had 0.150% (v/v) bovine pituitary extract (BPE) (Sigma, UK) and 0.02% (v/v) forskolin (Sigma, UK) added to their cell media. Cells were cultured in a humidified 37°C/5% CO<sub>2</sub>/95% air (v/v) environment.

Cells were grown to near confluence, and detached with 0.05% trypsin/EDTA (GIBCO, Invitrogen, Karlsruhe, Germany). A Neubauer chamber was used to count the cells. Passages 16-19 were used for dermal fibroblasts.

Inkjet printing was performed within 30 minutes of loading a cell suspension into the print reservoir. It was established from initial work by other research groups[32] and our experimentation that fibroblasts could be printed for up to 40 minutes without significant loss of cell number.

1 mL of fibroblasts were seeded at 40,000 cells/mL into each well, and topped off with 2 mL of cell media, before being stored in an incubator. The samples were experimented in triplicate, with light and confocal images taken on day 1, 2 and 3. Confocal images were stained with FITC-phalloidin and DAPI, with the aim to determine cell viability of these scaffolds.

For confocal fluorescence imaging, cells were seeded on the scaffolds at  $2 \times 10^4$  cells per sample, stained with phalloidin-fluorescein isothiocyanate (FITC) for F-actin filaments and 4',6-diamidino-2-phenylindole dihydrochloride (DAPI) for nuclear staining.

Samples were fixed with 3.7% formaldehyde in PBS for 30 minutes at room temperature and permeabilised with 0.1% (v/v) Triton X-100 in PBS for 30 minutes. Phalloidin:FITC was added at 1:1000 in PBS in combination with DAPI at 1:1000 (300 nM) for 30 minutes, washed and stored in PBS at 4°C until imaging. Cells were washed with PBS (x3) for 5 minutes between each step.

Samples were imaged using an inverted Zeiss LSM 510 META confocal microscope, using an argon 30 mW ion laser (488 nm) for FITC excitation  $\lambda_{ex} = 495$  nm /  $\lambda_{em} = 521$  nm. Nuclei were visualized by two photon excitation using a Chameleon Ti-Sapphire tuneable laser for DAPI excitation  $\lambda_{ex}$  400 nm;  $\lambda_{em} = 460$  nm.

Image acquisition and analysis were carried out with Carl Zeiss Laser Scanning Systems LSM 510 software.



## Acknowledgements

The authors wish to thank Dr Jonathan Stringer of the University of Auckland for their kind assistance in the preparation of this manuscript.

## References

- [1] M. Théry, "Micropatterning as a tool to decipher cell morphogenesis and functions," *J. Cell Sci.*, vol. 123, pp. 4201–4213, 2010.
- [2] S. Kumar and P. R. LeDuc, "Dissecting the molecular basis of the mechanics of living cells," *Exp. Mech.*, vol. 49, pp. 11–23, 2009.
- [3] Y. Zhang, C. Tse, D. Rouholamin, and P. J. Smith, "Scaffolds for tissue engineering produced by inkjet printing," *Cent. Eur. J. Eng.*, vol. 2, no. 3, pp. 325–335, Jun. 2012.
- [4] C. S. Chen, M. Mrksich, S. Huang, G. M. Whitesides, and D. E. Ingber, "Geometric control of cell life and death," *Science*, vol. 276, pp. 1425–1428, 1997.
- [5] L. E. Dike, C. S. Chen, M. Mrksich, J. Tien, G. M. Whitesides, and D. E. Ingber, "Geometric control of switching between growth, apoptosis, and differentiation during angiogenesis using micropatterned substrates," *In Vitro Cell. Dev. Biol. Anim.*, vol. 35, pp. 441–448, 1999.
- [6] R. McBeath, D. M. Pirone, C. M. Nelson, K. Bhadriraju, and C. S. Chen, "Cell shape, cytoskeletal tension, and RhoA regulate stem cell lineage commitment," *Dev. Cell*, vol. 6, pp. 483–495, 2004.
- [7] C. C. W. Tse, S. S. Ng, J. Stringer, S. MacNeil, J. W. Haycock, and P. J. Smith, "Utilising Inkjet Printed Paraffin Wax for Cell Patterning Applications," *Int. J. Bioprinting*, vol. 2, no. 0, Jan. 2016.
- [8] S. Banerjee, R. Sknepnek, and M. C. Marchetti, "Optimal shapes and stresses of adherent cells on patterned substrates," *Soft Matter*, vol. 10, pp. 2424–30, 2014.
- [9] B. Geiger, J. P. Spatz, and A. D. Bershadsky, "Environmental sensing through focal adhesions," *Nat. Rev. Mol. Cell Biol.*, vol. 10, pp. 21–33, 2009.
- [10] G. Duclos, S. Garcia, H. G. Yevick, and P. Silberzan, "Perfect nematic order in confined monolayers of spindle-shaped cells," *Soft Matter*, vol. 10, pp. 2346–53, 2014.
- [11] C. Tse, R. Whiteley, T. Yu, J. Stringer, S. MacNeil, J. W. Haycock, and P. J. Smith, "Inkjet printing Schwann cells and neuronal analogue NG108-15 cells," *Biofabrication*, vol. 8, no. 1, p. 015017, Mar. 2016.
- [12] J. L. Drury and D. J. Mooney, "Hydrogels for tissue engineering: Scaffold design variables and applications," *Biomaterials*, vol. 24, no. 24, pp. 4337–4351, 2003.
- [13] A. J. Kuipers, G. H. Engbers, J. Krijgsveld, S. A. Zaaij, J. Dankert, and J. Feijen, "Cross-linking and characterisation of gelatin matrices for biomedical applications," *J. Biomater. Sci. Polym. Ed.*, vol. 11, no. 3, pp. 225–243, 2000.
- [14] E. Esposito, R. Cortesi, and C. Nazzari, "Gelatin microspheres: influence of preparation parameters and thermal treatment on chemico-physical and biopharmaceutical properties," *Biomaterials*, vol. 17, no. 20, pp. 2009–20, Oct. 1996.
- [15] K. W. Wissemann and B. S. Jacobson, "Pure gelatin microcarriers: synthesis and use in cell attachment and growth of fibroblast and endothelial cells," *In Vitro Cell. Dev. Biol.*, vol. 21, no. 7, pp. 391–401, 1985.
- [16] A. Ito, A. Mase, Y. Takizawa, M. Shinkai, H. Honda, K.-I. Hata, M. Ueda, and T. Kobayashi, "Transglutaminase-mediated gelatin matrices incorporating cell adhesion factors as a biomaterial for tissue engineering," *J. Biosci. Bioeng.*, vol. 95, no. 2, pp. 196–199, 2003.
- [17] a Paguirigan and D. J. Beebe, "Gelatin based microfluidic devices for cell culture," *Lab Chip*, vol. 6, no. 3, pp. 407–13, Mar. 2006.
- [18] C. H. Yao, B. S. Liu, C. J. Chang, S. H. Hsu, and Y. S. Chen, "Preparation of networks of gelatin and genipin as degradable biomaterials," *Mater. Chem. Phys.*, vol. 83, no. 2–3, pp. 204–208, 2004.
- [19] A. Bigi, G. Cojazzi, S. Panzavolta, N. Roveri, and K. Rubini, "Stabilization of gelatin films by crosslinking with genipin," *Biomaterials*, vol. 23, no. 24, pp. 4827–4832, 2002.
- [20] F. H. Lin, C. H. Yao, J. S. Sun, H. C. Liu, and C. W. Huang, "Biological effects and cytotoxicity of the composite composed by tricalcium phosphate and glutaraldehyde cross-linked gelatin," *Biomaterials*, vol. 19, no. 10, pp. 905–17, May 1998.
- [21] H. W. Sung, D. M. Huang, W. H. Chang, R. N. Huang, and J. C. Hsu, "Evaluation of gelatin hydrogel crosslinked with various crosslinking agents as bioadhesives: in vitro study," *J. Biomed. Mater. Res.*, vol. 46, no. 4, pp. 520–30, Sep. 1999.
- [22] G. Wollensak, H. Aurich, C. Wirbelauer, and S. Sel, "Significance of the riboflavin film in corneal collagen crosslinking," *J. Cataract Refract. Surg.*, vol. 36, no. 1, pp. 114–120, 2010.
- [23] Y.-C. Ou, C.-W. Hsu, L.-J. Yang, H.-C. Han, Y.-W. Liu, and C.-Y. Chen, "Attachment of Tumor Cells to the Micropatterns of Glutaraldehyde (GA)-Crosslinked Gelatin," vol. 20, no. 8, pp. 435–446, 2008.
- [24] A. P. McGuigan and M. V. Sefton, "Modular tissue engineering: Fabrication of a gelatin-based construct," *J. Tissue Eng. Regen. Med.*, vol. 1, no. 2, pp. 136–145, 2007.
- [25] A. Bigi, G. Cojazzi, S. Panzavolta, K. Rubini, and N. Roveri, "Mechanical and thermal properties of gelatin films at different degrees of glutaraldehyde crosslinking," *Biomaterials*, vol. 22, no. 8, pp. 763–768, 2001.
- [26] L. H. H. O. Damink, P. J. Dijkstra, M. J. A. Van Luyn, P. B. Van Wachem, P. Nieuwenhuis, and J. Feijen, "Glutaraldehyde as a crosslinking agent for collagen-based biomaterials," *J. Mater. Sci. Mater. Med.*, vol. 6, no. 8, pp. 460–472, 1995.
- [27] J. Alvarado, B. M. Mulder, and G. H. Koenderink, "Alignment of nematic and bundled semiflexible polymers in cell-sized confinement," *Soft Matter*, vol. 10, pp. 2354–64, 2014.
- [28] C. Tomba, C. Brañi, B. Wu, N. S. Gov, and C. Villard, "Tuning the adhesive geometry of neurons: length and polarity control," *Soft Matter*, vol. 10, pp. 2381–7, 2014.
- [29] P. J. F. Röttgermann, A. P. Alberola, and J. O. Rädler, "Cellular self-organization on micro-structured surfaces," *Soft Matter*, vol. 10, pp. 2397–404, 2014.
- [30] N. Hampe, T. Jonas, B. Wolters, N. Hersch, B. Hoffmann, and R. Merkel, "Defined 2-D microtissues on soft elastomeric silicone rubber using lift-off epoxy-membranes for biomechanical analyses," *Soft Matter*, vol. 10, pp. 2431–2443, 2014.
- [31] U. S. Schwarz, C. M. Nelson, and P. Silberzan, "Proteins, cells, and tissues in patterned environments," *Soft Matter*, vol. 10, no. 14, pp. 2337–40, Apr. 2014.
- [32] B. Lorber, W.-K. Hsiao, I. M. Hutchings, and K. R. Martin, "Adult rat retinal ganglion cells and glia can be printed by piezoelectric inkjet printing," *Biofabrication*, vol. 6, no. 1, p. 015001, Dec. 2013.

## Author Biography

Christopher Tse is a postdoctoral researcher at the University of Sheffield working with Dr Patrick Smith in researching applied inkjet printing. His PhD thesis researched the applications of inkjet printing in tissue engineering. He is currently researching the applications of inkjet printing on composites and electronics as well as continuing his research into tissue engineering.